Frontiers in Heat and Mass Transfer (FHMT), 18, 47 (2022)
DOI: 10.5098/hmt.18.47

Global Digital Central
ISSN: 2151-8629

Frontiers in Heat and Mass Transfer

Available at www.ThermalFluidsCentral.org

COMPARISON OF TRANSIENT CHARACTERISTICS OF A CENTRIFUGAL PUMP DURING FORWARD AND REVERSE STOPPING PERIODS

Y. L. Zhang[a], H. B. Lin[b], S. P. Li[b,*], J. J. Xiao[a], L. Zhang[c]

[a] *College of Mechanical Engineering, Quzhou University, Quzhou, Zhejiang, 324000, China;*
[b] *College of Mechanical and Electrical Engineering, Northeast Forestry University, Harbin, Heilongjiang, 150040, China*
[c] *Department of Application & Engineering, Zhejiang Institute of Economics and Trade, Hangzhou, Zhejiang, 310018, China;*

ABSTRACT

Centrifugal pumps need to be stopped in the case of closing valve sometimes due to some specific application requirements. This paper presents a numerical simulation of the unsteady flow inside a low specific speed centrifugal pump during closed-valve forward and reverse stopping process. The study results show that the average internal pressure gradually decreases during stopping periods. At the same blade radius, the pressure on working surface is significantly higher than the suction surface. The pressure gradually increases from the impeller inlet to the outlet. The simulation fully shows the transient flow characteristics inside the centrifugal pump during forward and reverse stopping period.

Keywords: *Centrifugal pump; Closed valve; Stopping; Forward and reverse rotation; Transient effect*

1. INTRODUCTION

As one of the most widely used turbomachinery, centrifugal pumps play an important role in nuclear power, petrochemicals, and power stations, etc. Among them, low specific speed centrifugal pumps have the advantages of high head (Zhang *et al*. (2011), Cui *et al*. (2013)).

The current research on centrifugal pumps is mainly focused on the analysis of internal and external characteristics, and the transient characteristics research on stopping process is also mainly focused on the evolution of external characteristics and internal flow field. Chalghoum *et al*. (2016) studied the dynamic behavior of the pump during startup and analyzed the effect of impeller diameter and number of vanes on pressure evolution. Farhadi *et al.* (2007) predicted transient characteristics during pump startup and concluded that variable rotational speed and flow rate of pump can lead to difficulties in pump startup. Omri *et al.* (2021) found that the transient hydraulic performance of the pump during startup is strongly influenced by the rotational acceleration of motor, flow inertia, and impeller geometry. Zhu *et al.* (2011) studied the start-up process of open impeller centrifugal pumps and found that the rotational speed affects the state of change of speed and pressure with start-up time. Feng *et al.* (2021) studied the transient process caused by centrifugal pump power failure and found that the transient process of centrifugal pump after power failure its transient process mainly experienced four modes: pump mode, brake mode, turbine mode and runaway mode. During the transient process, the characteristic parameters such as flow rate, impeller force, torque and speed change sharply and stabilize after the runaway state. Trivedi Chirag *et al.* (2014) studied the emergency shutdown of a hydraulic turbine runner under non-constant pressure loads and found that the amplitude of pressure fluctuations increases with the increase in runner speed. Fu *et al.* (2020) studied characteristic processes of transient fluids during pump start-up were studied experimentally and numerically. Long *et al.* (2020, 2020) investigated the difference in flow characteristics between the transient start-up process and the steady state at the same speed at the corresponding moment under closed-valve transition and open-valve transition, and the difference in flow characteristics between the transient start-up process and the steady state at the same flow rate at the corresponding moment for variable-flow open valves; the transient fluid-solid coupling method was used to solve the transient internal flow and structural fields of the segmented multistage centrifugal pump during the closed-valve start-up process, and it was found that the radial and axial forces of the impeller were close to zero in the initial stage of the closed-valve transition start-up process. As the start-up process develops, the radial and axial forces of the impeller gradually increase, and the radial force fluctuates sharply with time, but the overall radial force is consistent at different stages. Li *et al.* (2018) performed numerical calculations of the internal flow field in a mixed-flow pump using a sliding grid method to investigate the pressure, flow line and relative velocity during start-up, providing an optimization theory to reveal the internal unsteady flow characteristics of mixed flow. Wang *et al.* (2019) studied the transient characteristics of an ultra-low ratio pump and found that the motor speed increases linearly at startup in the off state with different acceleration rates and reaches its highest value at the end of startup; as the starting acceleration increases, the vibration acceleration amplitude also increases with the main frequency. By comparing and analyzing the dynamic grid method, sliding grid method and dynamic reference system method, Wu *et al.* (2012, 2014) found that the sliding grid method has higher computational efficiency and computational accuracy in solving the three-dimensional transient flow of hydraulic machinery under transient conditions such as start-up and shutdown; the effect of the pump shutdown mode on the transient flow and pump characteristics for the piping system was studied, and it was found that the fluid flow and circuit during pump shutdown. It is found that the fluid flow and the duration of the circuit during pump stop is affected by the inertia of the pump rotor and the fluid inertia. Moreover, some

* *Corresponding author. Email: lisanping73@nefu.edu.cn*

Global Digital Central
ISSN: 2151-8629

transient behavior is also found in other classical flow (Abed *et al.* (2020), Gu *et al*. (2020)).

In view of the lack of research theories on transient flow in the shutdown process of closed-valve forward and reverse shutdown of centrifugal pumps, it is of great theoretical significance and engineering application value to analyze the transient hydraulic and structural dynamic characteristics in the shutdown process of closed-valve forward and reverse shutdown for the safety and reliability of multistage centrifugal pump operation. By establishing the fluid domain model of the whole centrifugal pump, the transient operation process of the closed valve forward and reverse stages are simulated numerically to reveal the change of external characteristics with time and the evolution characteristics of the internal flow field in the two transient operation processes. By comparing the external and internal flow fields of the transient process in the two phases with those of the same speed and flow rate at the corresponding time, the difference in flow characteristics between the transient process of the closed-valve forward and reverse shutdown process and the corresponding time at the constant state is explained, and the influence of the transient effect on the hydraulic performance in the two phases is investigated. In this paper, we propose to numerically simulate the internal flow field of a low specific speed centrifugal pump during the fast shutdown process of closed valve forward and reverse rotation, in order to grasp the basic characteristics of the changes in the transient process.

2. NUMERICAL SIMULATION METHODS

2.1 Computational Models

The pump used for the numerical simulation is a low specific speed centrifugal pump with a specific speed of 45. The design parameters and main dimensions of the centrifugal pump are seen from literature (Zhang *et al.* (2017), Cheng and Zhang (2022)). The vane profile adopts the double arc cylindrical form, the worm shell size change law adopts the Archimedes spiral form.

2.2 Mesh Division

GAMBIT software was used for meshing, in which unstructured tetrahedral mesh was used for the impeller and worm housing regions, and structured hexahedral mesh was used for the other calculation domains. After checking, the equirectangular slope and equidimensional slope of the mesh are less than 0.85, and the mesh quality is good. The number of meshes in the model was checked for correlation and found to be grid-independent when the variation of the external properties was less than 2%, and the total number of meshes in the computational domain was 508792. Figure 1 shows the computational domain grid, the front cover grid is not shown in the impeller on the right side.

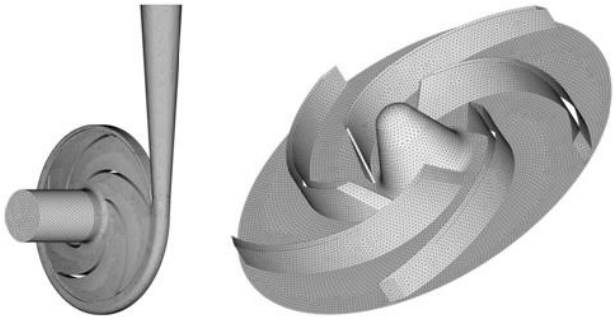

Fig. 1 Calculation grid

2.3 Solving For Control

A commercial computational software FLUENT 6.3 based on the finite volume method is used for the numerical calculation of a fully three-dimensional, incompressible, non-constant, viscous fluid. During the start-up process, the Reynolds number changes rapidly from zero to millions, and the flow changes rapidly from laminar flow in the initial stage to turbulent flow with very large changes in various flow modes. In this paper, the RNG turbulence model of the vortex-viscous model, which was proposed by Yakhot and Orzag in 1986, has been widely proven to be very effective for internal pump flows, and it can better handle flows with high strain rate and large degree of streamline curvature. The speed variation of the impeller is loaded using a user-defined function. The motor speed variation increases approximately exponentially during the start-up process

$$n = n_{\max} e^{-t/t_0} \tag{1}$$

$n_{\max}$ is the maximum speed, which is 1450rpm in this paper, $t_0 = 0.15$.

Since the valve is closed, the through flow is zero. In this paper, velocity inlet conditions and free outflow boundary conditions are used. Considering the viscous reason, the no-slip boundary condition is used at the wall, and the standard wall function method is used in the low Reynolds number region near the wall to deal with the problems caused by the high Reynolds number turbulence model. The time discretization of the transient term is in first-order implicit format, the spatial discretization of the convective term is in first-order windward format, the spatial discretization of the diffusive term is in central difference format with second-order accuracy, and the spatial discretization of the source term is in linearized standard format. The coupling of velocity and pressure is implemented using the SIMPLE algorithm. The default under-relaxation factor is used for all variables in the iterative calculations. The time step is taken as 0.001s and the start time is 1s. The maximum number of iterations in each time step is set to 40 (actual calculations show that this setting can guarantee the computational convergence in each time step) and the residual convergence accuracy is 0.001.

3. ANALYSIS OF RESULTS

3.1 External Characteristics Prediction

The numerical simulation of the centrifugal pump in forward and reverse rotation with the outlet valve closed was carried out separately, and the numerical simulation of the total inlet pressure in both states is shown in Fig. 2. The values, oscillation amplitude and fluctuation trend of the total inlet pressure in both cases of closed valve forward and reverse rotation are approximately equal within 1.2s of shutdown of the centrifugal pump with the outlet valve closed. And as the stopping time increases, the total inlet pressure in forward and reverse rotation shows an oscillating downward trend. Within 0.25s at the beginning of the shutdown process, the fluctuation of the total positive and reverse inlet pressure is large and keeps oscillating continuously, which may be caused by the chaotic internal flow field and complex flow of internal secondary flow at the initial stage of shutdown; within 0.25s to 0.45s, the fluctuation of the total positive and reverse inlet pressure decreases and shows a trend of decreasing in value; after 0.45s, the total positive and reverse inlet and outlet pressure gradually tends to be 0.

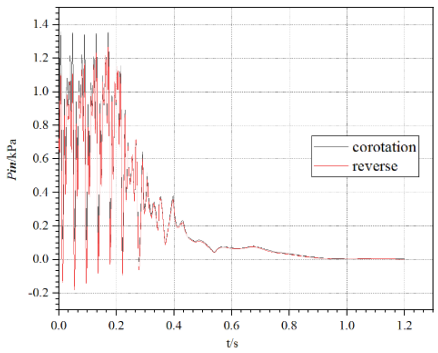

Fig. 2 Comparison of forward and reverse inlet total pressure

Global Digital Central
ISSN: 2151-8629

Figure 3 represents the variation curve of the total outlet pressure of the centrifugal pump in forward and reverse rotation within 1.2s of shutdown when the outlet valve is closed. Similar to the inlet total pressure, the values, oscillation amplitude and fluctuation trend of the outlet total pressure in both cases of forward and reverse rotation with the valve closed are approximately equal. In the first 0.2s of the shutdown process, the forward and reverse total outlet pressure fluctuated sharply from 8.0KPa to 10.1KPa; as the shutdown process continued, the forward and reverse total inlet pressure showed a significant oscillation downward trend from 8.579KPa in 0.2s to 0.130KPa in 0.6s, and the oscillation amplitude decreased gradually with the increase of time. The amplitude of oscillation gradually decreases with time. After 0.6s, the fluctuation of the total pressure at the forward/reverse outlet tends to stabilize, and the total pressure at the forward/reverse outlet tends to 0.

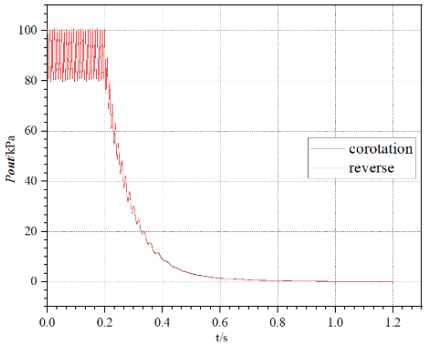

Fig. 3 Comparison of forward and reverse outlet total pressure

Figure 4 gives the variation curve of the forward and reverse head of the centrifugal pump within 0.8s of shutdown when the outlet valve is closed. The head values, oscillation amplitude and fluctuation trend are approximately equal for both cases of forward and reverse rotation with the valve closed. During the first 0.18s of the shutdown process, the values of the forward and reverse heads are in the range of 8.01m~10.12m, and the fluctuation amplitude is large; in the time 0.18s ⩽t⩽ 0.7s, the positive and negative head show a fluctuation down trend as the shutdown process continues, and the fluctuation amplitude gradually decreases with the increase of time until the fluctuation disappears. After 0.7s, the forward and reverse head tends to be horizontally stable, and tends to be 0 in value and finally.

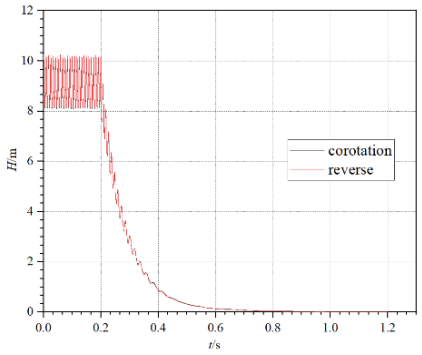

Fig. 4 Comparison of forward and reverse head

Figure 5 shows the change curve of forward and reverse impeller power during 1.2s of shutdown when the outlet valve is closed in the centrifugal pump. With the reduction of impeller speed after shutdown, the impeller power tends to an overall decreasing trend. As shown in the figure, the values, oscillation amplitude and fluctuation trend of impeller power are approximately equal in both cases of forward and reverse rotation with the valve closed. In the first 0.2s of the shutdown process, the impeller power values of forward and reverse rotation are oscillating at 200W~300W; in the time 0.2s⩽t⩽ 0.3s, the impeller power of forward and reverse rotation decreases sharply and the fluctuation amplitude increases gradually: in 0.3s~0.5s, as the shutdown process continues, the impeller power of forward and reverse rotation increases gradually and tends to 0, and the fluctuation amplitude also disappears gradually. After 0.5s, the forward and reverse impeller power is kept at 0.

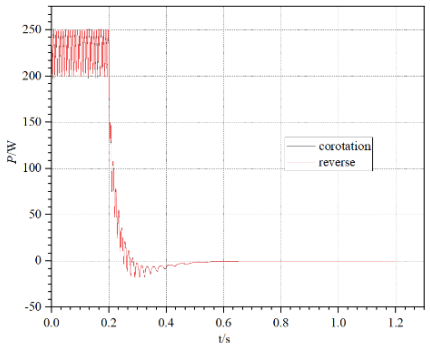

Fig. 5 Forward and reverse impeller power comparison

Figure 6 shows that the impeller dynamic reaction force fluctuates greatly during the first 0.18s in the closed-valve shutdown impeller reaction force at the outlet of the centrifugal pump. As shown in the figure, the impeller dynamic reaction force oscillates with a large amplitude between -0.7N and 2.2N in the closed-valve forward rotation condition; in the reverse rotation condition, the impeller dynamic reaction force oscillates with a large amplitude between -0.5N and 2.35N. After 0.18s in the shutdown process, the impeller dynamic reaction force in forward and reverse rotations showed a trend of decreasing fluctuation. As the shutdown process continues, the positive and negative impeller dynamic reaction force gradually tends to 0, and the fluctuation amplitude also gradually disappears.

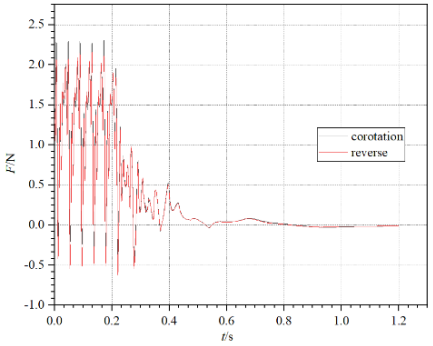

Fig. 6 Comparison of dynamic reaction force of forward and reverse impeller

3.2 Flow Field Analysis

The cloud diagram of the total pressure evolution during the shutdown of the centrifugal pump with the outlet valve closed is shown in Fig. 7, which shows the total pressure evolution distribution at eight discrete time points of the internal flow field during the shutdown. At the moment of shutdown, the internal pressure of the centrifugal pump increases gradually along the radial direction from the impeller hub to the inner wall of the casing due to the impeller working. Meanwhile, at the same radius of the impeller, the pressure on the pressure surface of the impeller is significantly higher than that on the suction surface, and the high pressure area is concentrated at the trailing edge of the impeller blades. In the six discrete time points from 0s to 0.16s during the shutdown process, the pressure inside the flow field from the inlet to the outlet of the impeller shows an increasing trend. After 0.16s at the beginning of shutdown, the internal flow field tends to be stable, and the pressure at each place inside the flow field is equal.

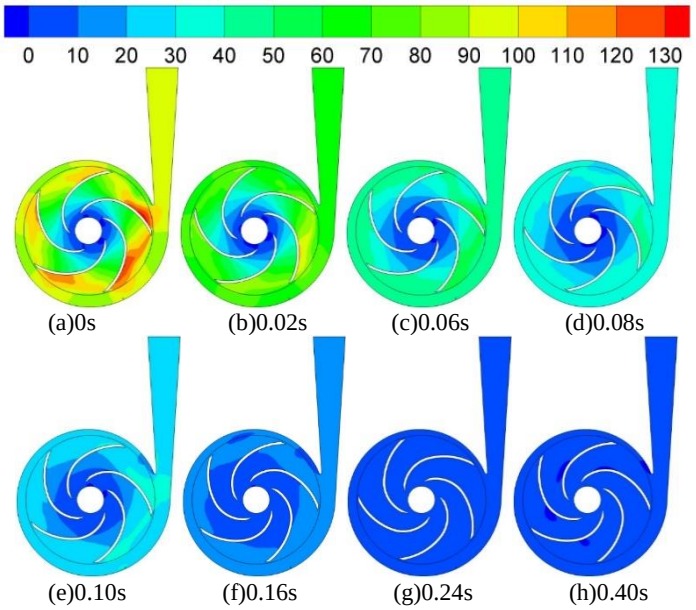

Fig. 7 Evolution of total pressure during positive rotation shutdown

In order to better reveal the transient characteristics of the centrifugal pump shutdown process in the closed valve state, simulations were performed at different times after the shutdown, and the transient flow distribution at eight discrete time points were obtained, as shown in Fig. 8. At different time points during the shutdown process, the trend of transient flow lines inside the centrifugal pump with decreasing speed is basically the same, but there are large differences in the distribution of flow fields under different shutdown stages. In the initial moment of shutdown, the internal flow distribution is relatively uniform and the internal flow velocity at the outlet is larger; as the shutdown process continues (0s⩽t⩽0.08s), the internal flow velocity shows a gradual weakening trend with the reduction of impeller speed. Starting from 0.10s after the start of shutdown, the vortex area appears at the inlet of the impeller runner, and the distribution area of the vortex gradually becomes larger with the decrease of the rotational speed in 0.10s⩽t⩽0.40s. The vortex area at the inlet of the impeller runner becomes larger in a small way, and the internal flow field is chaotic until the pump stops and gradually disappears in the runner.

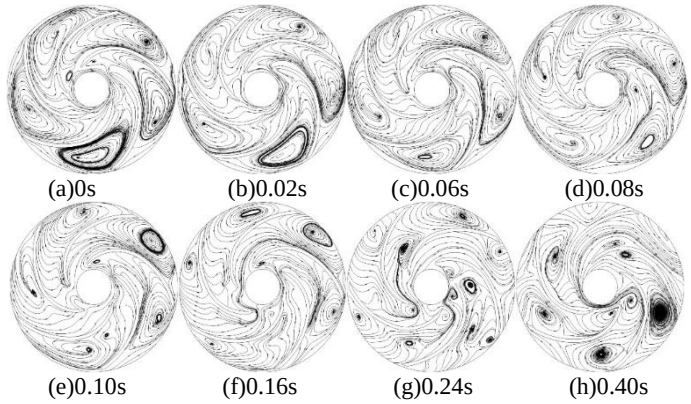

Fig. 8 Transient flow line evolution during positive rotation shutdown

The static pressure distribution of the internal flow field during the reversal shutdown is obtained by numerical simulation, as shown in Fig. 9. The pressure is approximately equal at the same radius. The pressure at the blade surface gradually decreases along the streamline direction at the initial moment of shutdown because of the reduction of impeller speed. The pressure at the impeller pressure surface at each discrete time point is greater than the pressure at the suction surface, and the low pressure area is mainly distributed at the edge of the impeller shaft, and the high pressure area is mainly concentrated at the inner wall of the pump casing; the pressure gradually increases from inside to outside as the radius increases. At the initial moment of the shutdown process, the pressure in the internal flow field gradually becomes larger from the inlet to the outlet, and the maximum pressure is concentrated at the outlet. In the 1s of the shutdown process, the internal flow field tends to stabilize and the pressure gradually decreases in all places.

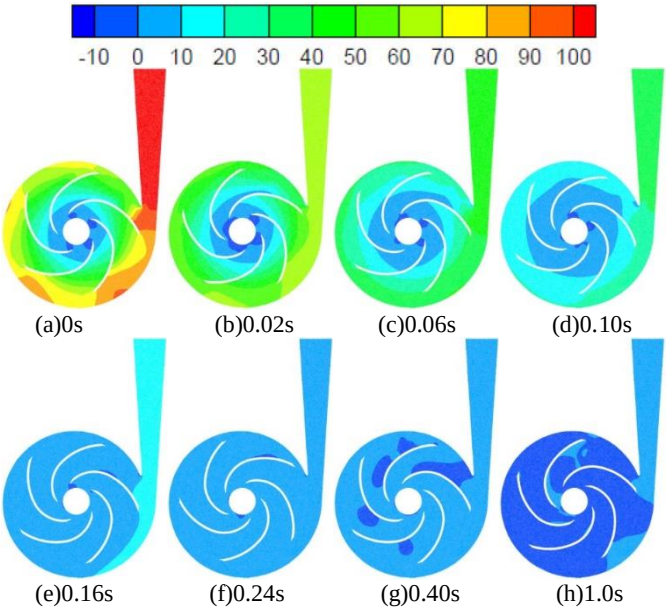

Fig. 9 Hydrostatic pressure evolution during reversal shutdown

Figure 10 shows the vortex distribution at eight discrete time points during the reversal shutdown process. At the initial moment of the shutdown process, the vortex distribution inside the centrifugal pump is large and the internal flow field is active; the high vortex values are concentrated at the vane pressure surface, and the vortex values increase along the trailing edge of the vane. From the overall view of the eight discrete time points, the vortex value gradually decreases with the continuation of the shutdown process; in 0.6s⩽t⩽0.40s, the internal flow field gradually stabilizes, and the high vortex value is mainly concentrated at the spacer tongue.

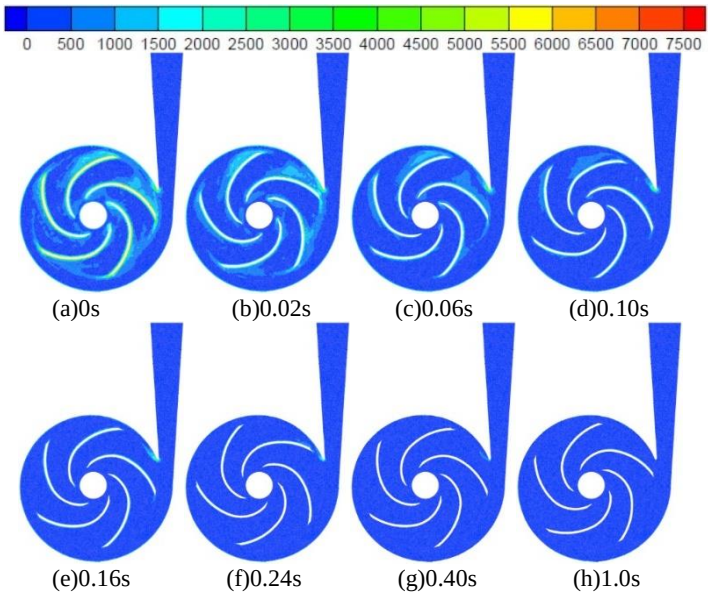

Fig. 10 Evolution of total pressure during positive rotation shutdown

Global Digital Central
ISSN: 2151-8629

4. CONCLUSION

This paper use numerical simulation technology to study the non-constant flow of the internal flow field during the shutdown operation of a centrifugal pump in the closed valve state, and initially grasp the basic change characteristics during this transient process. The conclusions of this paper are as follows:

(1) In the shutdown process of centrifugal pump with closed valve forward and reverse, the total inlet and outlet pressure, head, impeller power and impeller dynamic reaction force in the two cases of forward and reverse are roughly equal in value, oscillation amplitude and fluctuation trend; in the initial moment of shutdown, the total inlet and outlet pressure, head, impeller power and impeller dynamic reaction force oscillate strongly in value, and show oscillation down trend with the continuation of the shutdown process, and eventually tends to zero.

(2) Using multiple discrete time points to analyze the internal flow field of the centrifugal pump, it can be obtained that at the moment of positive rotation shutdown, the internal pressure of the centrifugal pump gradually increases along the radial direction from the impeller hub to the inner wall of the casing; and at the same radius of the impeller, the pressure on the impeller pressure surface is significantly higher than that on the suction surface, and the high pressure area is concentrated at the trailing edge of the impeller blades, while the low pressure area is mainly distributed at the edge of the impeller shaft.

(3) In the shutdown process at different time points, the trend of transient flow inside the centrifugal pump with the reduction of speed is basically the same. However, at the initial moment of shutdown, the internal flow distribution is relatively uniform and the internal flow velocity at the outlet is larger; within $0.10s \leqslant t \leqslant 0.40s$ during the shutdown process, the vortex area appears at the inlet of the impeller runner and gradually becomes larger with the reduction of rotational speed. The internal vortex distribution is large, and the high vortex value is concentrated at the spacer tongue and the pressure surface of the blade, and the vortex value increases along the trailing edge of the blade.

ACKNOWLEDGEMENTS

The research was financially supported by the National Natural Science Foundation of China (Grant No. 51876103), "Pioneer" and "Leading Goose" R&D Program of Zhejiang (Grant No. 2022C03170) and Zhejiang Provincial Natural Science Foundation of China (Grant No. LZY21E060001 and LZY21E060002).

REFERENCES

Abed, I.M., Ali, F.H., and Sahib, S.A.M., 2020, "Investigation of heat transfer and fluid flow around sinsoudal corrugated circular cylinder for two dimensional system," *Frontiers in Heat and Mass Transfer*, 15(6), 1-9.
http://dx.doi.org/10.5098/hmt.15.6.

Chalghoum, I., Elaoud, S., Akrout, M., and Taieb, E.H., 2016, "Transient behavior of a centrifugal pump during starting period," *Applied Acoustics*, 109, 82-89.
https://doi.org/10.1016/j.apacoust.2016.02.007

Cheng, L., and Zhang, Y.L., 2022, "Self-coupling numerical calculation of centrifugal pump startup process," *Frontiers in Heat and Mass Transfer*, 18(26), 1-6.
http://dx.doi.org/10.5098/hmt.18.26

Cui, B.L., Wang, C.F., Zhu, Z.C., and Jin, Y.Z., 2013, "Influence of blade outlet angle on performance of low-specific-speed centrifugal pump," *Journal of Thermal Science*, 22(02), 117-122.
https://doi.org/10.1007/s11630-013-0601-6

Farhadi, K., Bousbia-salah, A., and D'Auria, F., 2007, "A model for the analysis of pump start-up transients in tehran research reactor," *Progress in Nuclear Energy*, 49(7), 499-510.
https://doi.org/10.1016/j.pnucene.2007.07.006

Feng, J.J., Ge, Z.G., Zhang, Y., Zhu, G.J., Wu, G.K., Lu, J.L., and Luo, X.Q., 2021, "Numerical investigation on characteristics of transient process in centrifugal pumps during power failure," *Renewable Energy*, 170, 267-276.
https://doi.org/10.1016/j.renene.2021.01.104

Fu, S.F., Zheng, Y., Kan, K., Chen, H.X., Han, X.X., Liang, X.L., Liu, H.W., and Tian, X.Q., 2020, "Numerical simulation and experimental study of transient characteristics in an axial flow pump during start-up," *Renewable Energy*, 146, 1879-1887.
https://doi.org/10.1016/j.renene.2019.07.123

Gu, X., Jiang, G., Wo, Y., and Chen, B., 2020, "Numerical study on heattransfer characteristics of propylene glycole-water mixture in shell side of spiral wound heat exchanger," *Frontiers in Heat and Mass Transfer*, 15(3), 1-8.
http://dx.doi.org/10.5098/hmt.15.3.

Li, W., Zhang, Y., Shi, W.D., Ji, L.L., Yang, Y.F., and Ping, Y.F., 2018, "Numerical simulation of transient flow field in a mixed-flow pump during starting period," *International Journal of Numerical Methods for Heat & Fluid Flow*, 28(4), 927-942.
https://doi.org/10.1108/HFF-06-2017-0220

Long, Y., Lin, B., Fang, J., Ge, J., Xu, L.B., Fu, Q., and Zhu, R.S., 2020, "Research on the pump shaft stability analysis of multistage centrifugal pump during closed-valve start-up process," *Frontiers in Energy Research*, 8(186), 1-8.
https://doi.org/10.3389/fenrg.2020.00186

Long, Y., Lin, B., Fang, J., Zhu, R.S., and Fu, Q., 2020, "Research on the transient hydraulic characteristics of multistage centrifugal pump during start-up process," *Frontiers in Energy Research*, 8(76), 1-15.
https://doi.org/10.3389/fenrg.2020.00076

Omri, F., Hadj-Taieb, L., and Elaoud, S., 2021, "Numerical study on the transient behavior of a radial pump during starting time," *AQUA — Water Infrastructure, Ecosystems and Society*, 70(3), 257-273.
https://doi.org/10.2166/aqua.2021.136

Trivedi, C., Cervantes, M.J., Gandhi, B.K., and Dahlhaug, O.G., 2014, "Transient pressure measurements on a high head model francis turbine during emergency shutdown, total load rejection, and runaway," *Journal of Fluids Engineering*, 136(12), 107-121.
https://doi.org/10.1115/1.4027794

Wang, Y., Xie, L., Chen, J., Liu, H.L., Luo, K.K., Zhang, Z.L., and Cao, M.H., 2019, "Experimental study on transient startup characteristics of a super low specific speed centrifugal pump," *JOURNAL OF CHEMICAL ENGINEERING OF JAPAN*, 52(9), 743-750.
https://doi.org/10.1252/jcej.19we042

Wu, D.Z., Wu, P., Yang, S., and Wang, L.Q., 2014, "Transient characteristics of a closed-loop pipe system during pump stopping periods," *Journal of Pressure Vessel Technology*, 136(2), 21-31.
https://doi.org/10.1115/1.4025616

Zhang, Y.L., Zhu, Z.C., Dou, H.S., Cui, B.L., Li, Y., and Zhou, Z.Z., 2017, "Numerical investigation of transient flow in a prototype centrifugal pump during startup period," *International Journal of Turbo & Jet-Engines*, 34(2), 167-176.
https://doi.org/10.1515/tjj-2015-0064

Zhang, Y.X., Zhou, X., Ji, Z.L., and Jiang, C.W., 2011, "Numerical design and performance prediction of low specific speed centrifugal pump impeller," *International Journal of Fluid Machinery and Systems*, 4(1), 133-139.
https://doi.org/10.5293/IJFMS.2011.4.1.133

Global Digital Central
ISSN: 2151-8629

Zhu, Z.C., Guo, X.M., Cui, B.L., and Li, Y., 2011, "External characteristics and internal flow features of a centrifugal pump during rapid startup," *Chinese Journal of Mechanical Engineering*, 24(05), 798-804.
https://doi.org/10.3901/CJME.2011.05.798

Wu, D.Z., Chen, T., Sun, Y.B., Li, Z.F., and Wang, L.Q., 2012, "A study on numerical methods for transient rotating flow induced by starting blades," *International Journal of Computational Fluid Dynamics*, 26(5), 297-312.
https://doi.org/10.1080/10618562.2012.715154